Supporting information

Conductive hydrogels with ultra-stretchability and adhesiveness for flame- and cold-tolerant strain sensors

Cuiwen Liu,[a] Ru Zhang,[a] Peiwen Li,[a] Jinqing Qu,[b] Pengjie Chao,[a] Zongwen Mo,[a] Tao Yang,[a] Ning Qing,[a,*] Liuyan Tang[a,*]

[a] School of Biotechnology and Health Sciences, Wuyi University, Jiangmen, 529020, China

[b] School of Chemistry and Chemical Engineering, South China University of Technology, Guangzhou 510640, China

*Corresponding author.

E-mails: wyuchemtangly@126.com (Liuyan Tang), wyuchemqn@126.com (Ning Qing)

Table S1. Varied weight percentage of L ($L_{wt\%}$) in the hydrogels.

Sample	AAm (mg)	L (mL)	DI water (mL)	$L_{wt\%}$
L_0-$P_{(0.7,24\ h)}$-G_{50}	250	0	1	0
L_6-$P_{(0.7,24\ h)}$-G_{50}		0.2	0.8	6
L_{12}-$P_{(0.7,24\ h)}$-G_{50}		0.4	0.6	12
L_{18}-$P_{(0.7,24\ h)}$-G_{50}		0.6	0.4	18
L_{24}-$P_{(0.7,24\ h)}$-G_{50}		0.8	0.2	24
L_{30}-$P_{(0.7,24\ h)}$-G_{50}		1	0	30

*All samples were fabricated using 2.0 mg APS (step one), 2 μL TMEDA, 0.68% mass ratio of MBAA to AAm, 0.7 molar ratio of PA to Py, 136.9 mg APS (step two) and 50 vol% glycerol. The soaking time in PA/Py mixed solution was 24 h.

Table S2. Varied PA/Py molar ratio in the hydrogels.

Sample	PA/ Py (mol%)	soaking time in PA/ Py mixed solution (h)	APS(step two) (mg)	$G_{vol\%}$
L_{18}-$P_{(0,24\ h)}$-G_{50}	0	24	136.9	50
L_{18}-$P_{(0.5,24\ h)}$-G_{50}	0.5			
L_{18}-$P_{(0.7,24\ h)}$-G_{50}	0.7			
L_{18}-$P_{(1.4,24\ h)}$-G_{50}	1.4			

*All samples were fabricated using 250 mg AAm, 2.0 mg APS (step one), 0.67 wt% of MBAA to AAm, 2 μL TMEDA and 18 wt% L.

Table S3. Varied soaking time of the hydrogels in PA/Py mixed solution.

Sample	PA/ Py (mol%)	soaking time in PA/ Py mixed solution (h)	APS(step two) (mg)	$G_{vol\%}$
L_{18}-$P_{(0.7,6\ h)}$-G_{50}	0.7	6	136.9	50
L_{18}-$P_{(0.7,\ 12\ h)}$-G_{50}		12		
L_{18}-$P_{(0.7,24\ h)}$-G_{50}		24		
L_{18}-$P_{(1.4,\ 48\ h)}$-G_{50}		48		

*All samples were fabricated using 250 mg AAm, 2.0 mg APS (step one), 0.67 wt% of MBAA to AAm, 2 μL TMEDA and 18 wt% L.

Table S4. Varied volume percentage of glycerol ($G_{vol.\%}$) in the hydrogels.

Sample	PA/ Py (molar ratio)	APS (step two) (mg)	Glycerol (ml)	DI water (ml)	$G_{vol\%}$
L_{18}-$P_{(0.7,24\ h)}$-G_0	0.7	136.9	0	1	0
L_{18}-$P_{(0.7,24\ h)}$-G_{30}			0.3	0.7	30
L_{18}-$P_{(0.7,24\ h)}$-G_{50}			0.5	0.5	50
L_{18}-$P_{(0.7,24\ h)}$-G_{70}			0.7	0.3	70

*All the samples were fabricated using 250 mg AAm, 2.0 mg APS (step one), 0.67 wt% of MBAA to AAm, 2 μL TMEDA and 18 wt% L. The soaking time in PA/Py mixed solution was 24 h.

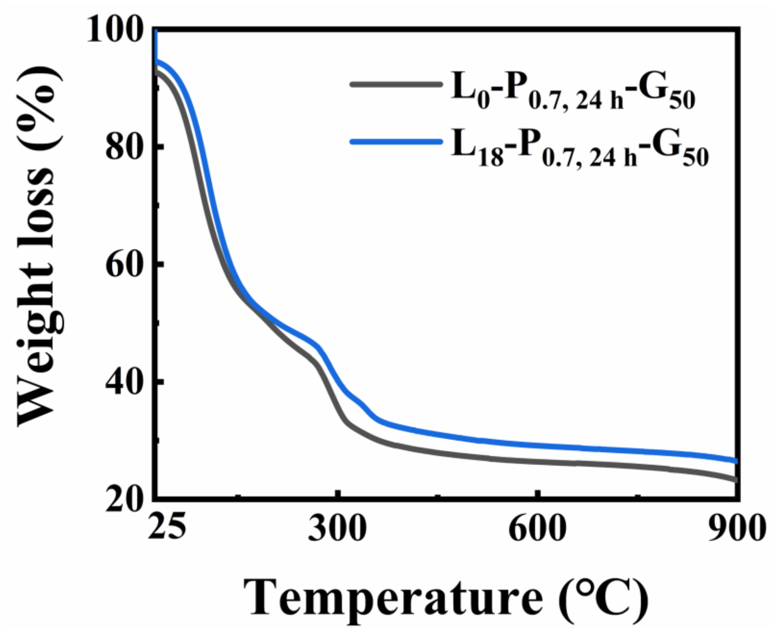

Figure S1. The TGA analysis of L_0-$P_{(0.7,24\ h)}$-G_{50} and L_{18}-$P_{(0.7,24\ h)}$-G_{50}.

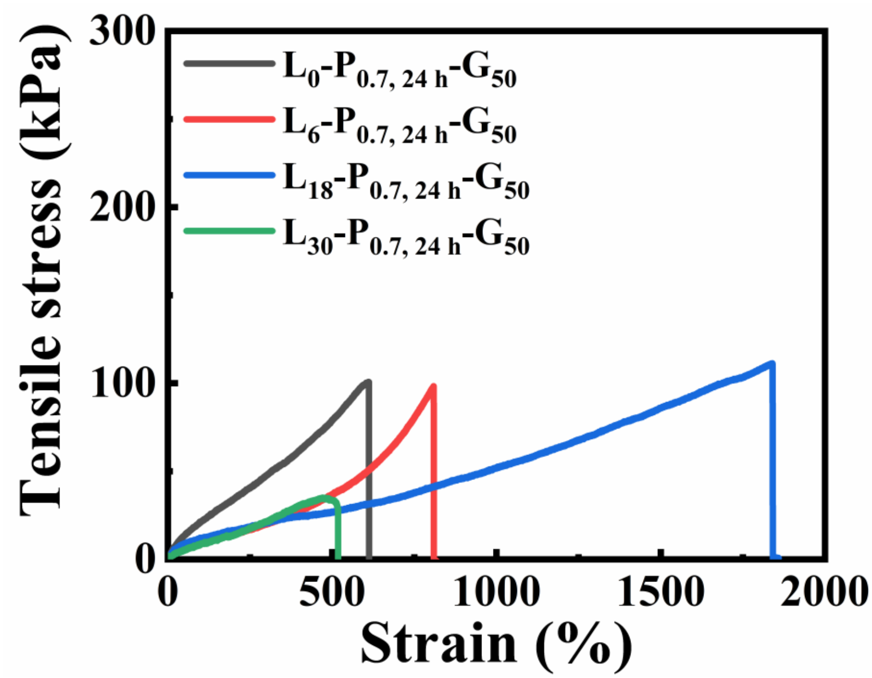

Figure S2. Uniaxial tensile test results of the hydrogels with different $L_{wt\%}$.

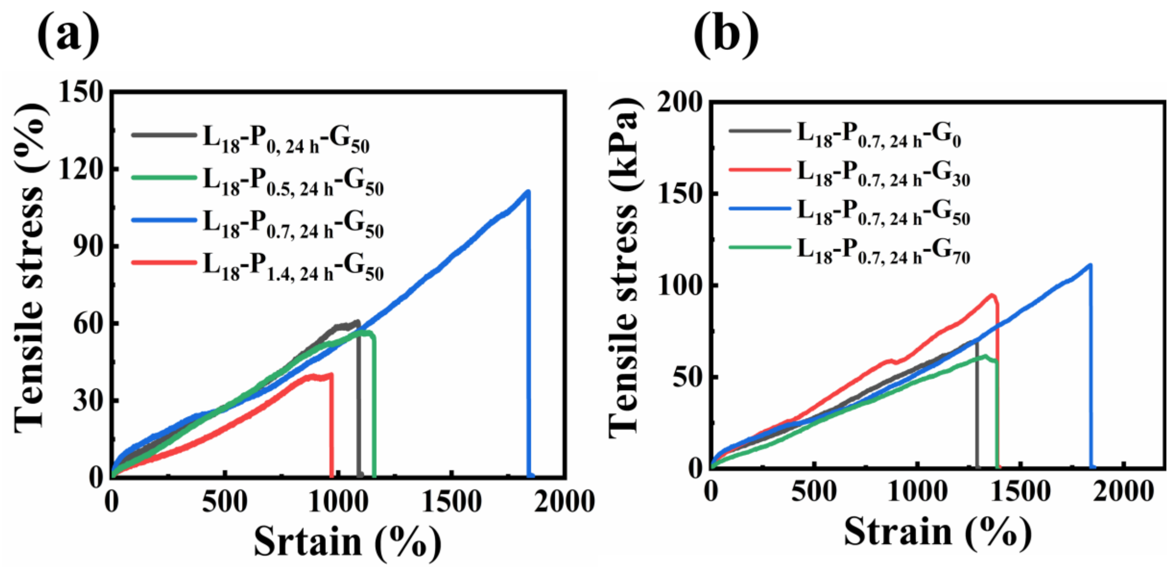

Figure S3. Uniaxial tensile test results of the hydrogels with varied (a) molar ratio of PA to Py and (b) volume ratio of glycerol.

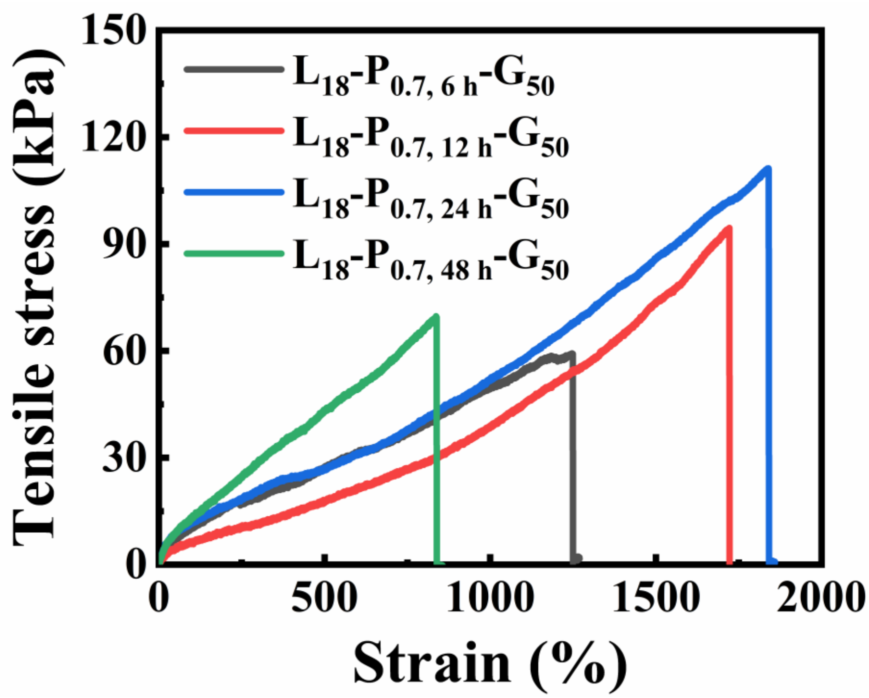

Figure S4. Uniaxial tensile test results of the hydrogels with different soaking time in the PA/Py mixed solution.

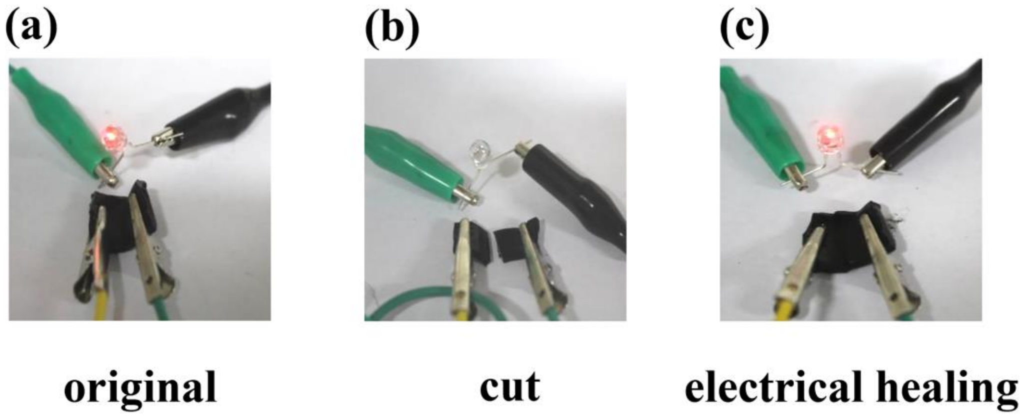

Figure S5. A circuit comprising a L_{18}-$P_{(0.7,\ 24\ h)}$-G_{50} strip in series with a red LED indicator: (a) original, (b) completed cut and (c) electrical healing.

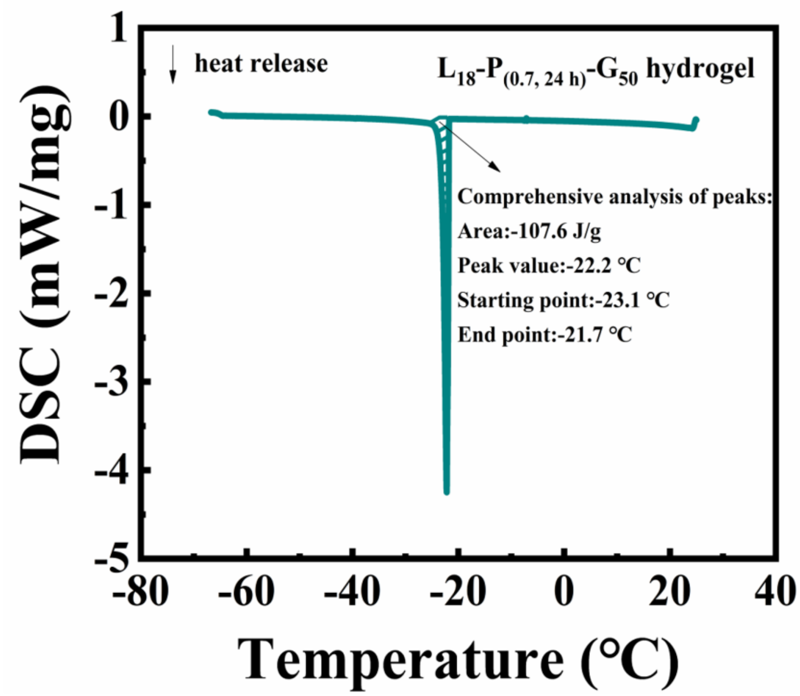

Figure S6. DSC curve of L_{18}-$P_{(0.7,\ 24\ h)}$-G_{50}.

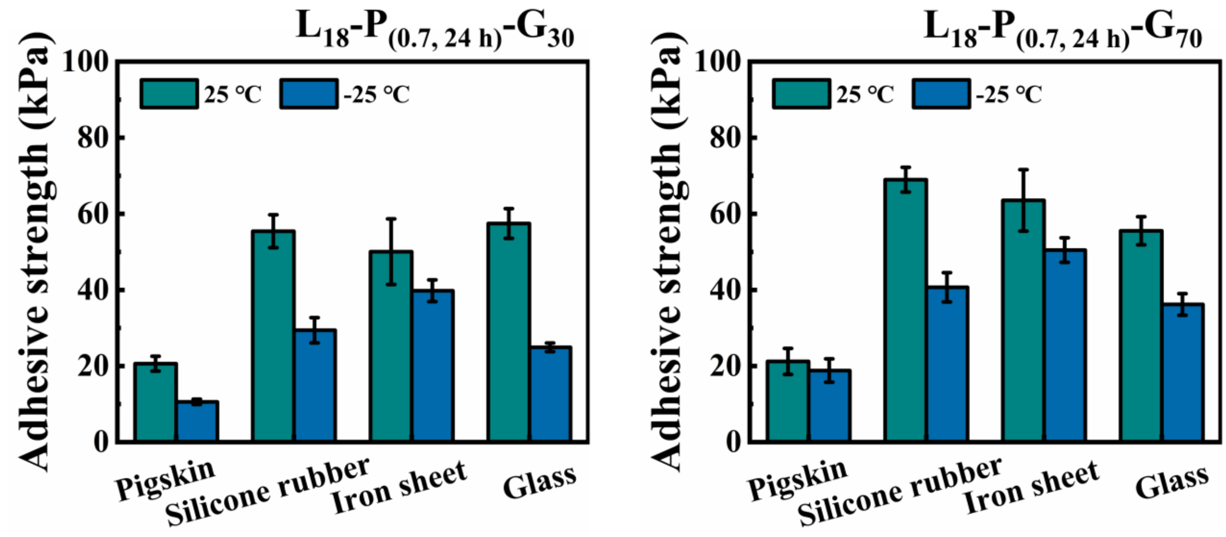

Figure S7. The adhesive strength of L_{18}-$P_{(0.7,\ 24\ h)}$-G_{30} and L_{18}-$P_{(0.7,\ 24\ h)}$-G_{70} on various subtracts at 25 ℃ and -20 ℃.

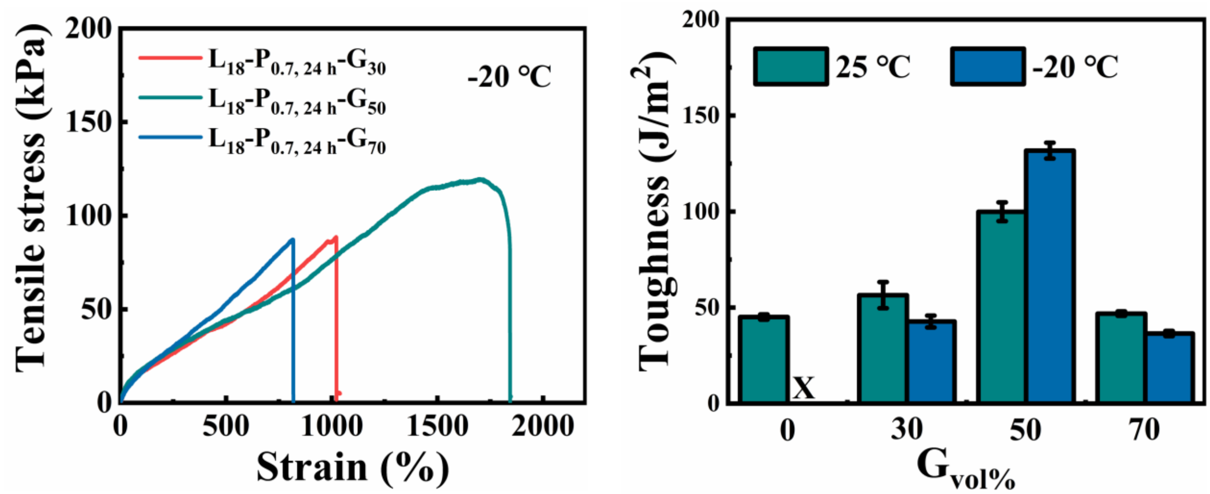

Figure S8. Uniaxial tensile test results of the hydrogels with different volume ratio of glycerol at -20 ℃ (left), and the relative toughness (right).

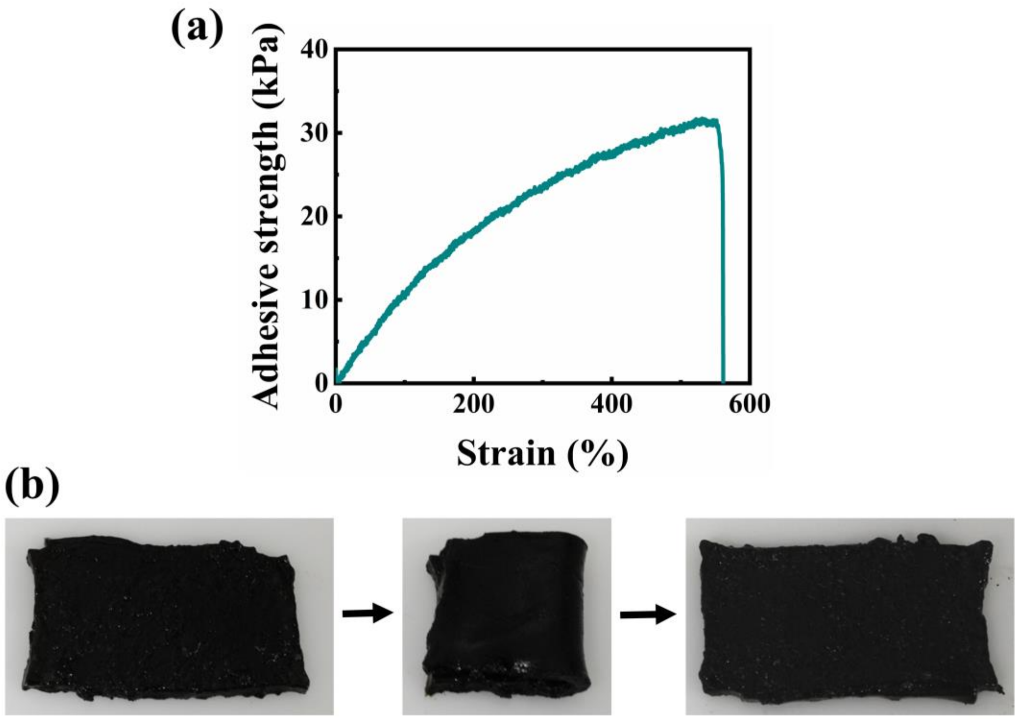

Figure S9. (a) the adhesive strength conducting by directly bonding of two pieces of L_{18}-$P_{(0.7, 24 h)}$-G_{50}. (b) The fold and recovery of a strip shaped L_{18}-$P_{(0.7, 24 h)}$-G_{50} sample.

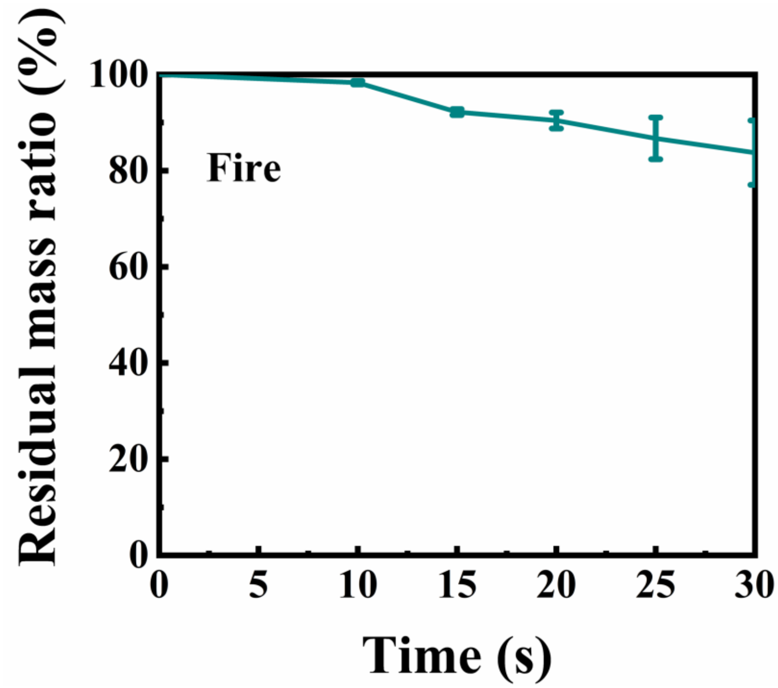

Figure S10. The solvent loss of L_{18}-$P_{(0.7,\ 24\ h)}$-G_{50} burning by alcohol lamp.

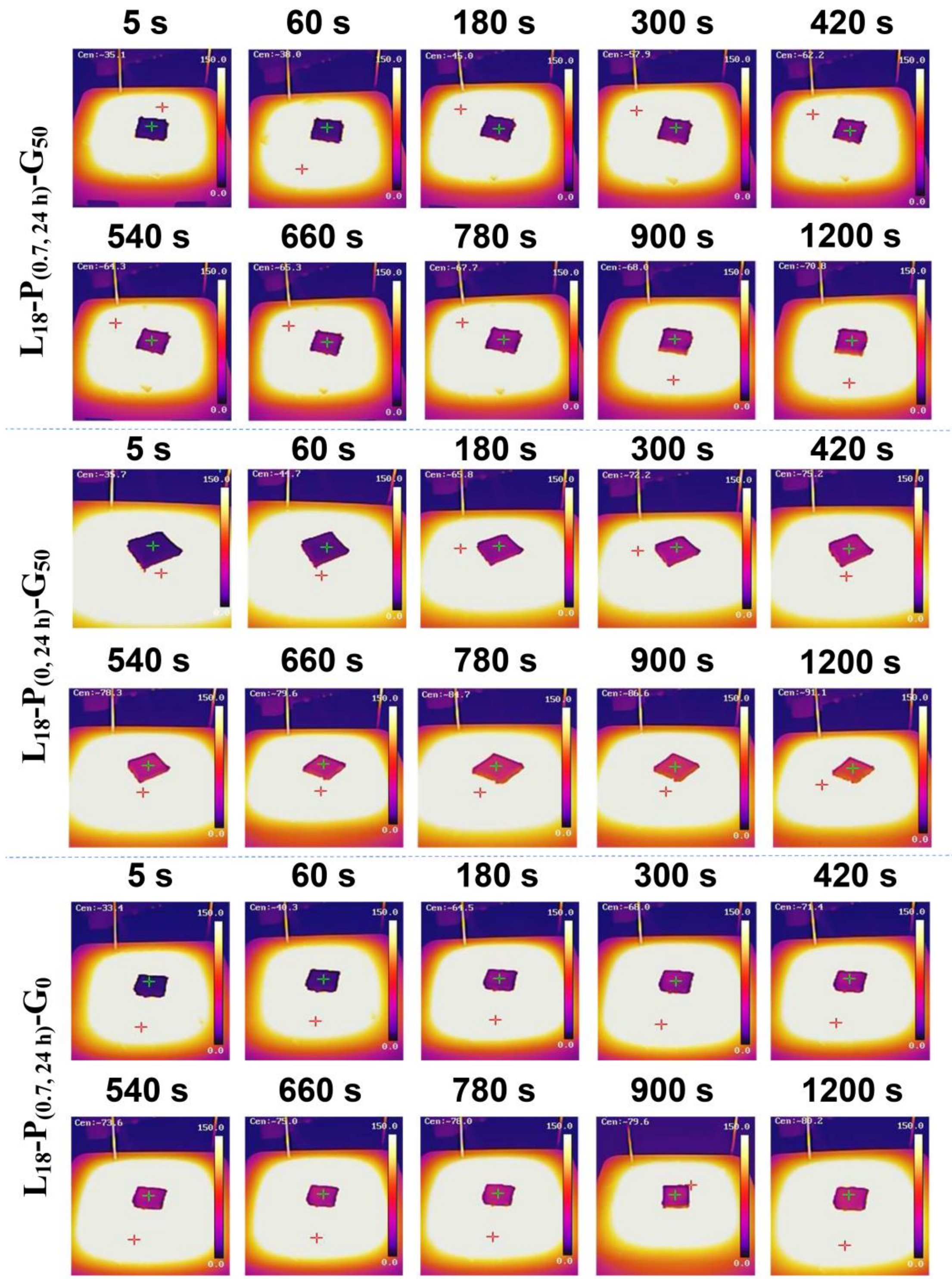

Figure S11. Infrared thermal images of L_{18}-$P_{(0.7,\ 24\ h)}$-G_{50}, L_{18}-$P_{(0,\ 24\ h)}$-G_{50} and L_{18}-$P_{(0.7,\ 24\ h)}$-G_0 placed on a hotplate with a pre-set surface temperature at 200 °C.

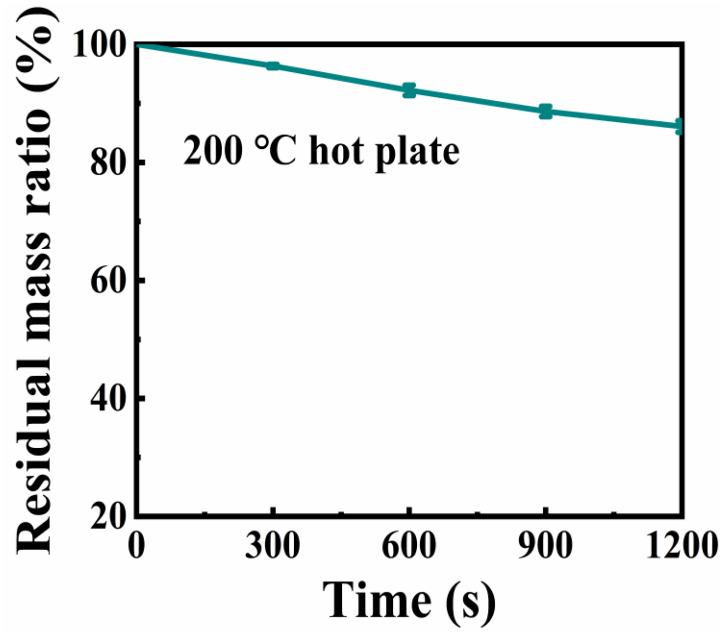

Figure S12. The solvent loss of L_{18}-$P_{(0.7,\ 24\ h)}$-G_{50} placed on a hotplate with a pre-set surface temperature at 200 °C.

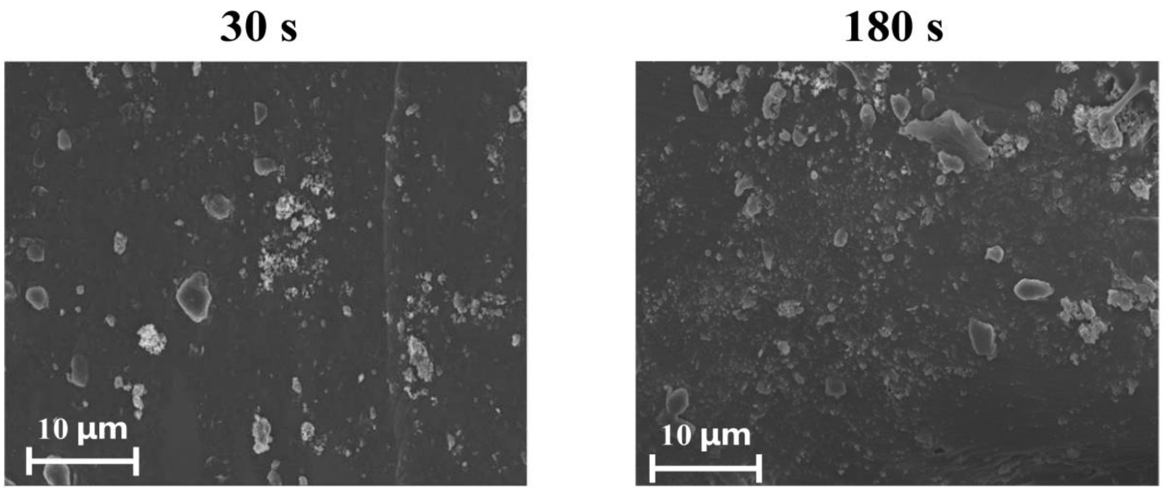

Figure S13. SEM images of L_{18}-$P_{(0.7,\ 24\ h)}$-G_{50} after burning for 30 s and 180 s.

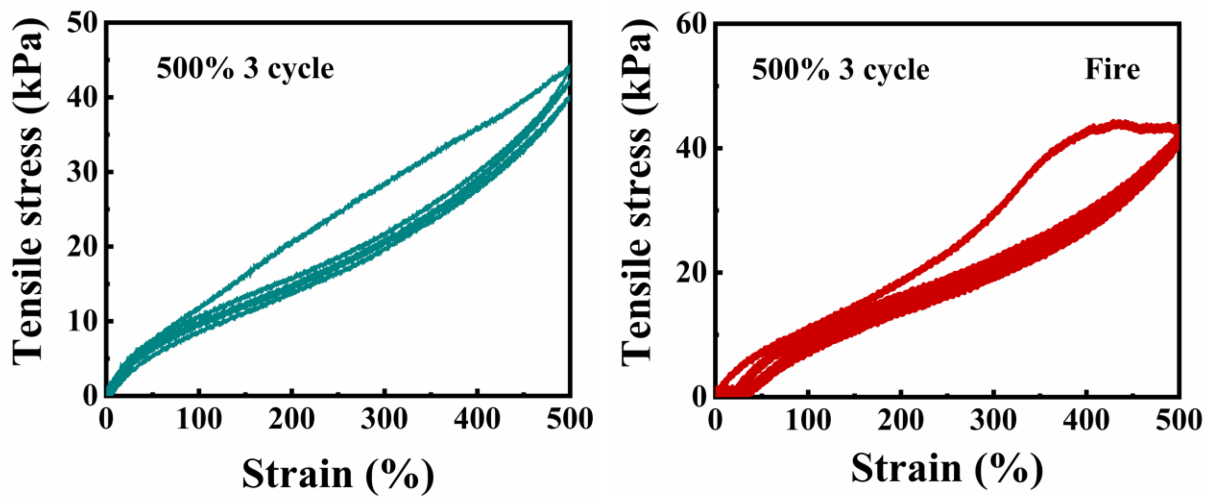

Figure S14. Cyclic loading–unloading curves of L_{18}-$P_{(0.7,\ 24\ h)}$-G_{50} at 25 °C and after burning for 30 s under a strain of 500% for 3 cycles.

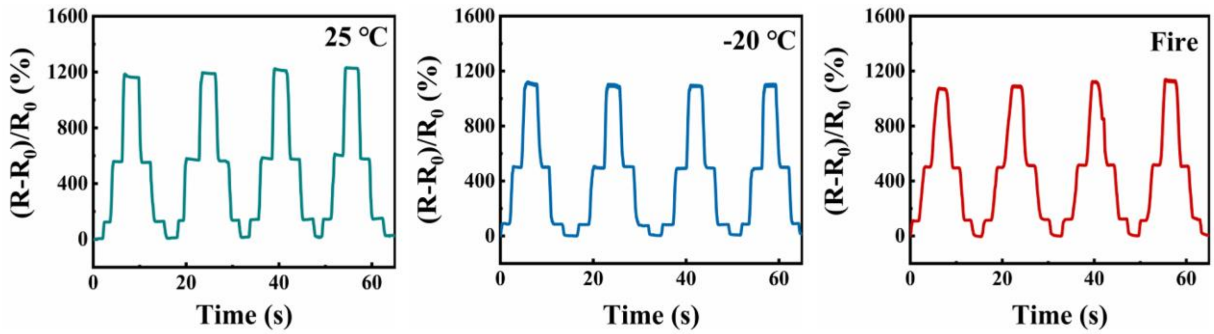

Figure S15. Relative resistance variations of the strain sensors at different elongations (100%, 300% and 500%), the cycles are repeated 3 times.

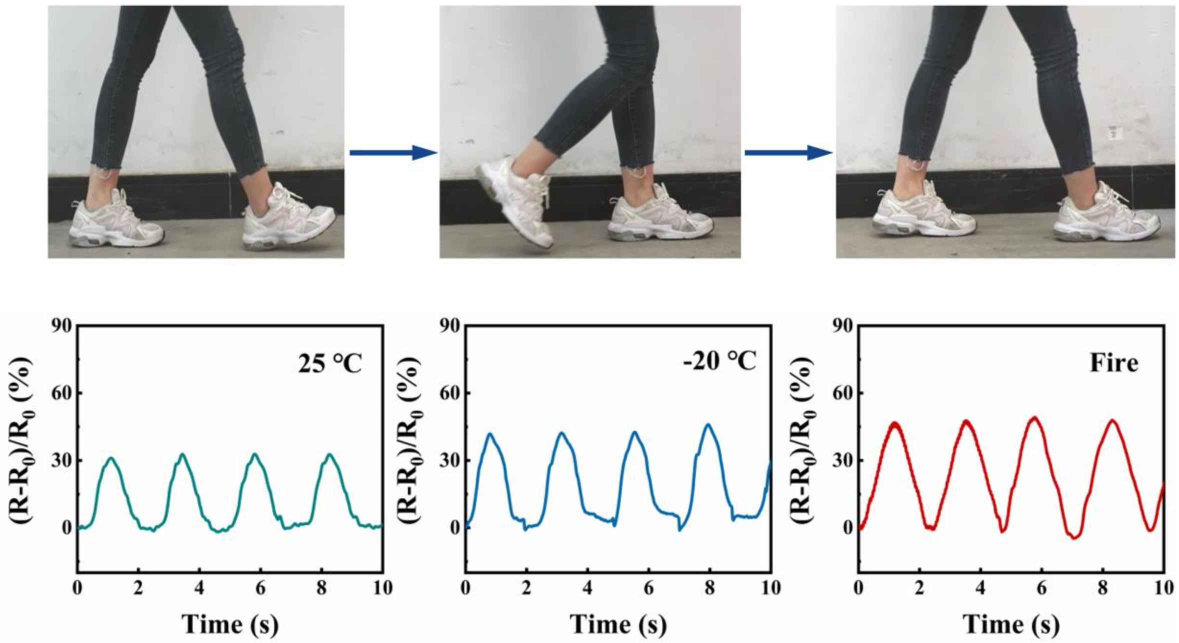

Figure S16. The resistance changes of the sensor for monitoring walking by knee joint bending at 25 °C, -20 °C and after burning for 30 s.

Table S5. A comparison on the properties of this work with other adhesive hydrogel sensors.

Ref.	Adhesive Strength (KPa)		Temperature Resistance (°C)	Maximum Fracture Strain (%)	Gauge Factor	Working Ranges (%)	Stable Sensing at Cold and High Temperature
	maximum	on skin					
[1]	26.8	26.8	-14~65	1200	2.50	0~100	No
[2]	8.9	3.7	-30~40	~600	1.93	0~300	No
[3]	45.3	14.2	-40~25	1124	2.22	0~170	No
					3.32	170~310	
					4.53	310~500	
[4]	24.3	NA	-14~60	1029	0.5	0~100	No
					1.2	100~900	
[5]	26.0	12.6	-20~100	1089	3.91	0~250	No
					8.82	250~100	
[6]	~23	~9	R.T.	~1100	1.66	0~650	No
[7]	5.9	5.9	R.T.	400	0.75	0~40	No
[8]	~12	NA	R.T.	680	0.60	0~20	No
					1.28	20~50	
					5.10	50~500	
[9]	~65	NA	R.T.	1600	0.6	0~20	No
					1.23	20~50	
					5.86	50~500	
[10]	~1.4	0.7	R.T.	140	1.68	0~100	No
[11]	5.5	~2	R.T.	1500	0.5~0.6	0~50	No
					0.8~1.4	125~220	
[12]	9.9	5.9	R.T.	~900	2.55	0~500	No
[13]	57.8	NA	R.T.~150	720	1.85	0~100	No
This work	79.7	26.9	-20~Fire (~600 °C)	1896	1.70	0~250	Yes
					2.90	250~500	

NA: not applicable.

References:

(1) He, Z.; Yuan, W. Adhesive, Stretchable, and Transparent Organohydrogels for Antifreezing, Antidrying, and Sensitive Ionic Skins. *ACS Appl. Mater. Interfaces* **2021**, *13* (1), 1474–1485.

(2) Zhang, X.; Cui, C.; Chen, S.; Meng, L.; Zhao, H.; Xu, F.; Yang, J. Adhesive Ionohydrogels Based on Ionic Liquid/Water Binary Solvents with Freezing Tolerance for Flexible Ionotronic Devices. *Chem. Mater.* **2022**, *34* (3), 1065–1077.

(3) Cao, L.; Zhao, Z.; Li, J.; Yi, Y.; Wei, Y. Gelatin-Reinforced Zwitterionic Organohydrogel with Tough, Self-Adhesive, Long-Term Moisturizing and Antifreezing Properties for Wearable Electronics. *Biomacromolecules* **2022**.

(4) He, Z.; Yuan, W. Highly Stretchable, Adhesive Ionic Liquid-Containing Nanocomposite Hydrogel for Self-Powered Multifunctional Strain Sensors with Temperature Tolerance. *ACS Appl. Mater. Interfaces* **2021**, *13* (44), 53055–53066.

(5) Zhou, H.; Lai, J.; Zheng, B.; Jin, X.; Zhao, G.; Liu, H.; Chen, W.; Ma, A.; Li, X.; Wu, Y. From Glutinous-Rice-Inspired Adhesive Organohydrogels to Flexible Electronic Devices Toward Wearable Sensing, Power Supply, and Energy Storage. *Adv. Funct. Mater.* **2022**, *32* (1), 2108423.

(6) Zheng, H.; Lin, N.; He, Y.; Zuo, B. Self-Healing, Self-Adhesive Silk Fibroin Conductive Hydrogel as a Flexible Strain Sensor. *ACS Appl. Mater. Interfaces* **2021**, *13* (33), 40013–40031.

(7) Lei, H.; Zhao, J.; Ma, X.; Li, H.; Fan, D. Antibacterial Dual Network Hydrogels for Sensing and Human Health Monitoring. *Adv. Healthc. Mater.* **2021**, *10* (21), 1–13.

(8) Li, Y.; Gong, Q.; Liu, X.; Xia, Z.; Yang, Y.; Chen, C.; Qian, C. Wide Temperature-Tolerant Polyaniline/Cellulose/Polyacrylamide Hydrogels for High-Performance Supercapacitors and Motion Sensors. *Carbohydr. Polym.* **2021**, *267* (April), 118207.

(9) Yu, X.; Zheng, Y.; Zhang, H.; Wang, Y.; Fan, X.; Liu, T. Fast-Recoverable, Self-Healable, and Adhesive Nanocomposite Hydrogel Consisting of Hybrid Nanoparticles for Ultrasensitive Strain and Pressure Sensing. *Chem. Mater.* **2021**, *33* (15), 6146–6157.

(10) Zhao, M.; Zhang, W.; Wang, D.; Sun, P.; Tao, Y.; Xu, L.; Shi, L. A Packaged and Reusable Hydrogel Strain Sensor with Conformal Adhesion to Skin for Human Motions Monitoring. *Adv. Mater. Interfaces* **2021**, 2101786.

(11) Wu, S.; Shao, Z.; Xie, H.; Xiang, T.; Zhou, S. Salt-Mediated Triple Shape-Memory Ionic Conductive Polyampholyte Hydrogel for Wearable Flexible Electronics. *J. Mater. Chem. A* **2021**, *9* (2), 1048–1061.

(12) Zhao, W.; Zhang, D.; Yang, Y.; Du, C.; Zhang, B. A Fast Self-Healing Multifunctional Polyvinyl Alcohol Nano-Organic Composite Hydrogel as a Building Block for Highly Sensitive Strain/Pressure Sensors. *J. Mater. Chem. A* **2021**, *9* (38), 22082–22094.

(13) Cho, K. G.; An, S.; Cho, D. H.; Kim, J. H.; Nam, J.; Kim, M.; Lee, K. H. Block Copolymer-Based Supramolecular Ionogels for Accurate On-Skin Motion Monitoring. *Adv. Funct. Mater*. **2021**, *31* (36), 1–11.